AN ALTERNATE DESIGN TECHNIQUE FOR SQUARE ROOT NYQUIST SHAPING FILTERS

fred harris
San Diego State University
fred.harris@sdsu.edu

Chris Dick
Xilinx Corp.
chris.dick@xilinx.com

ABSTRACT

The convolution of shaping and matched square-root Nyquist filters leads to a parent Nyquist filter with equally spaced time domain zeros and with a smooth pass-band to stop-band taper. When this taper is a cosine, the parent filter is a cosine tapered Nyquist filter and its children are the square root cosine tapered Nyquist filters. The cosine taper is the result of convolving a rectangle spectrum with a half cycle cosine spectrum. The half cycle cosine spectrum is not a good choice to form the filter's spectral taper. The square-root Nyquist filter produced from the cosine tapered Nyquist filter exhibit high levels of in-band ripple and insufficient out-of-band attenuation levels. Harry Nyquist off-handedly suggested that the half cycle cosine shape might make a good taper. It was an unfortunate off-hand remark that has burdened our community with poor performing shaping filters. The half cycle cosine is not sufficiently smooth to enable good square root Nyquist Filters. This paper presents a design technique, using smoother spectral shapes, to realize Square-Root Nyquist shaping filters with significantly reduced levels of spectral in-band ripple and improved out-of band attenuation levels.

Keywords: SQRT Nyquist, In-Band Ripple, Stop Band Attenuation

1. INTRODUCTION

The traditional cosine tapered Nyquist spectrum is obtained by convolving the ideal rectangle spectrum of width 1/T with a half cycle cosine shaped spectrum of width α/T. The equivalent process is the time domain product of the two time series representing the inverse transforms of the rectangle and inverse transform of the half cycle cosine. This frequency domain convolution process and the time domain product process are shown in (1) and (2).

$$H_{RC}(f) = \text{rect}(\frac{1}{T}) * \left\{ \frac{2\alpha}{\pi T} \cos(2\pi \frac{fT}{2\alpha}) \cdot \text{rect}(\frac{\alpha}{T}) \right\} \quad (1)$$

$$h_{RC}(t) = (\frac{1}{T}) \frac{\sin(\pi \frac{t}{T})}{(\pi \frac{t}{T})} \frac{\cos(\pi \frac{\alpha}{T} t)}{[1-(\frac{2\alpha}{T} t)^2]} \quad (2)$$

We note from (2) that the impulse response falls off as $1/t^3$ and does not have finite extent so we are obliged to apply a second window, the rectangle window, of length NT seconds to obtain finite length impulse responses. To obtain a Nyquist shaped communication signal at a receiver, the Nyquist filter is partitioned into a cascade of two filters. Each filter performs half the spectral shaping by implementing the square-root frequency response of the desired Nyquist Spectrum.

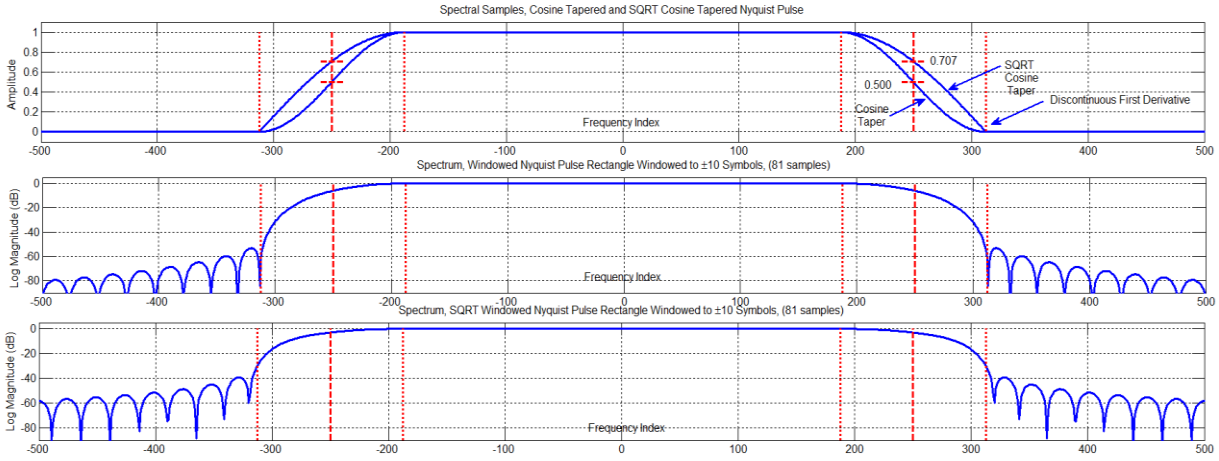

Figure 1. Cosine Tapered and SQRT Cosine Tapered Spectral Template and Spectra of Cosine Tapered and SQRT Tapered 81-Tap Filter Implementations: 4-Samples per Symbol, α=0.25

We do this to obtain the Nyquist spectral shape at the receiver while simultaneously maximizing the receiver's SNR by matching the receiver filter to the modulation shaping filter as shown in (3a) and (3b).

$$H_{RC}(f) = H_{SHAPE}(f) \cdot conj\{H_{SHAPE}(f)\}\exp(-j2\pi f T_{DLY}) \quad (3a)$$

$$H_{RC}(f) = |H_{SHAPE}(f)|^2 \cdot \exp(-j2\pi f T_{DLY})$$

$$H_{SHAPE}(f) = \sqrt{H_{RC}(f)}\ \exp(-j2\pi f T_{DLY}/2) \quad (3b)$$

Figure 1 showed the frequency response templet and log-magnitude spectrum of the Cosine Tapered (Raised Cosine, RC) Nyquist filter implemented as an 81-tap filter spanning 20 modulation symbols. Figure 1 also showed the frequency response template and log magnitude spectrum of Square-Root Cosine Tapered (SR-RC) Nyquist filter. Note that the spectral gain at the band edge of the RC Nyquist filter is 0.5 or -6 dB while the spectral gain at the band edge of the SR-RC Nyquist filter is SQRT(0.5) or -3 dB. Note also the discontinuous derivative of the SQRT spectrum. This discontinuity is responsible for the large out-band spectral sidelobes seen in figure 1. There is a piecewise continuous closed form description of the SR-RC Nyquist filter spectrum and similarly a closed form description of the SR-RC Nyquist filter time response. The time response is shown in (4). Here we again note that the impulse response falls off as $1/t^3$ and we have to truncate this impulse response with the rectangle window.

$$h_{SR-RC}(t) = \frac{2\alpha}{\pi\sqrt{T_{sym}}} \frac{(4\alpha\frac{t}{T_{sym}})\cos[(1+\alpha)\pi\frac{t}{T_{sym}}] + \sin[(1-\alpha)\pi\frac{t}{T_{sym}}]}{(4\alpha\frac{t}{T_{sym}})[1-(4\alpha\frac{t}{T_{sym}})^2]} \quad (4)$$

DESIGN APPROACH

The high levels of in-band ripple and high level out-of band side lobe filter responses are traceable to the lack of smoothness, or lack of multiple zeros, at the boundary of the spectral pulse convolved with the Nyquist spectrum prior to the square-r

oot operation of the smoothed spectrum. The insufficiently smooth spectral pulse results in high levels of time response side lobes which in turn, when truncated lead to high levels of spectral in-band and out-of band side lobes. Figure 2 shows a smooth spectral taper with multiple boundary zeros with the same 25% width as the shown half cosine spectral taper. The convolution of the two taper options result in the two spectra shown in subplot 2 and the SQRT of these tapered spectra is shown in subplot 3. Figure 3 shows the impulse response of the harris tapered and cosine tapered SQRT Nyquist filters along with an expanded view of their low-level side lobes. The significant reduction in side lobe levels holds the promise of improved performance SQRT Nyquist filters. Figure 4 compares SQRT Nyquist filters of length 40 symbols designed with the cosine taper and the harris taper. We show the two impulse responses and on one subplot show their spectral out-of band stop-band responses levels and again on another subplot show their spectral in-band pass-band ripple levels. We see the harris taper filter exhibits about an order of magnitude additional stop band attenuation over the Cosine taper filter as well as an order of magnitude reduction of in-band ripple level.

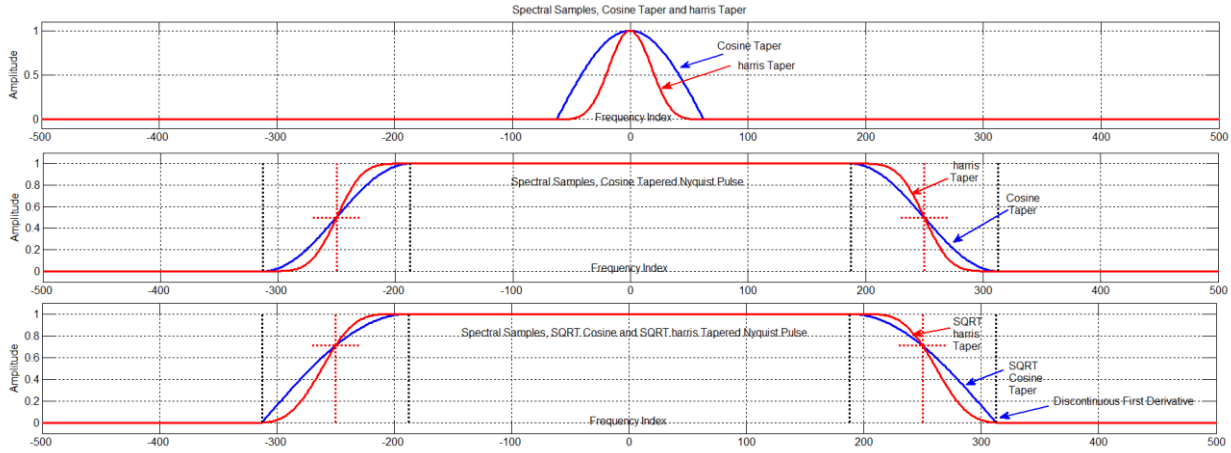

Figure 2 Cosine and harris Tapers, Cosine and harris Tapered Nyquist Spectra, and Cosine and harris SQRT Tapered Spectra

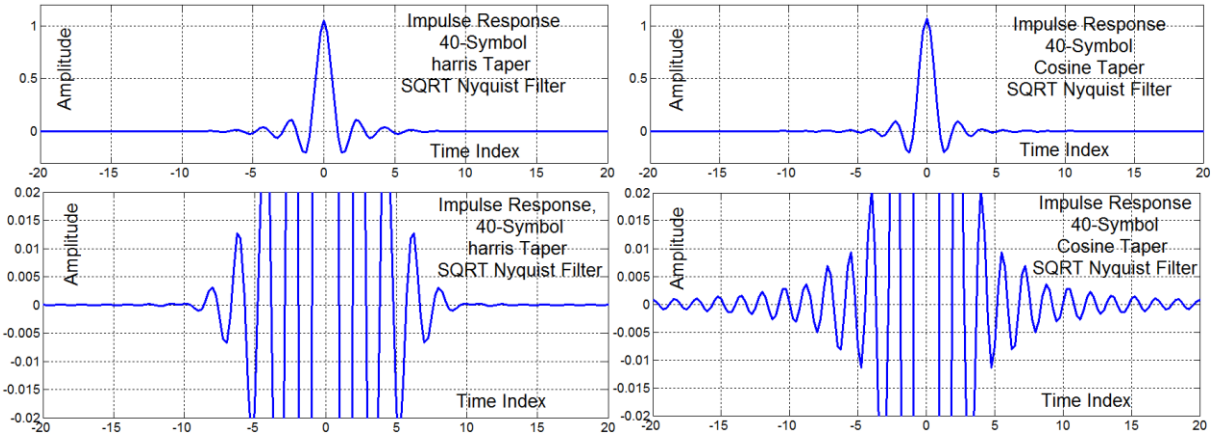

Figure 3. Comparison of Low level Time Domain Side Lobes of harris Tapered and Cosine Tapered SQRT Nyquist Pulses

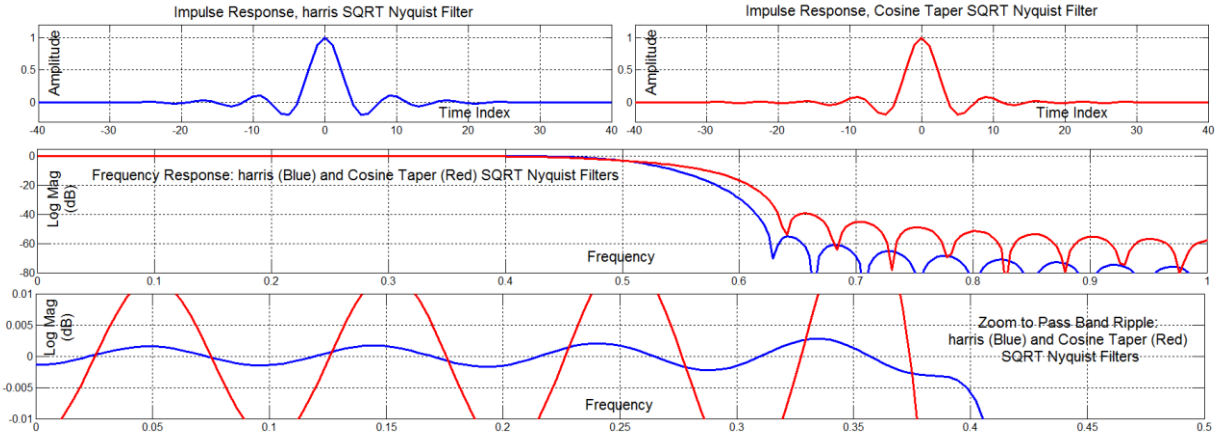

Figure 4. Comparison of 40-Symbol harris Taper and Cosine Taper SQRT Nyquist Filters: Time Responses, Stop-Band Frequency Responses, and In-Band Ripple Level Responses.

Figure 5 shows the correlation function or composite impulse response of shaping filter and matched filter for the two SQRT Nyquist filters which synthesize a Nyquist filter response. The bottom two subplots show the details of the expected zero-crossings which by their deviation from zero are the cause of ISI induced by the in-band ripple responses. We clearly see here the large levels of pre and post echo levels from the cosine taper filter as well as the rather small levels of deviation from zero exhibited by the harris taper filters.

Figure 6 shows the eye diagrams and the constellations formed by random QPSK modulated shaping and matched filtering of the two SQRT Nyquist filters. The zoom to the maximum eye opening time spot of the eye diagrams clearly show the reduced level of ISI by the harris taper filters relative to the cosine taper filters. Similarly, the zoom to the constellation cluster shows the order of magnitude reduction in cluster spreading offered by the harris taper SQRT Nyquist filter over that offered by the cosine taper SQRT Nyquist filter.

3. DESIGN PROCESS

The design of the alternate SQRT Nyquist filter proceeds as follows. We start with filter specifications defining number of samples per symbol and alpha, the fractional excess bandwidth. We form an array containing frequency domain samples of the rectangle bandwidth and of the taper to be convolved with the rectangle. The new design replaces the cosine half cycle taper with the harris taper, one that exhibits improved time domain sidelobes.

The question now is how to design the harris taper? The taper is simply a good spectral window with a span determined by the excess bandwidth and the number of samples spanning the frequency array. As a specific example, suppose we start the design with a 2000 point frequency array and a design specification of 4-samples per symbol and 25% excess bandwidth. We would then assign 500 samples to the target passband and 125 samples to the taper. We then select or design a smooth window with narrow mainlobe width and low sidelobe levels. We all have experience designing such

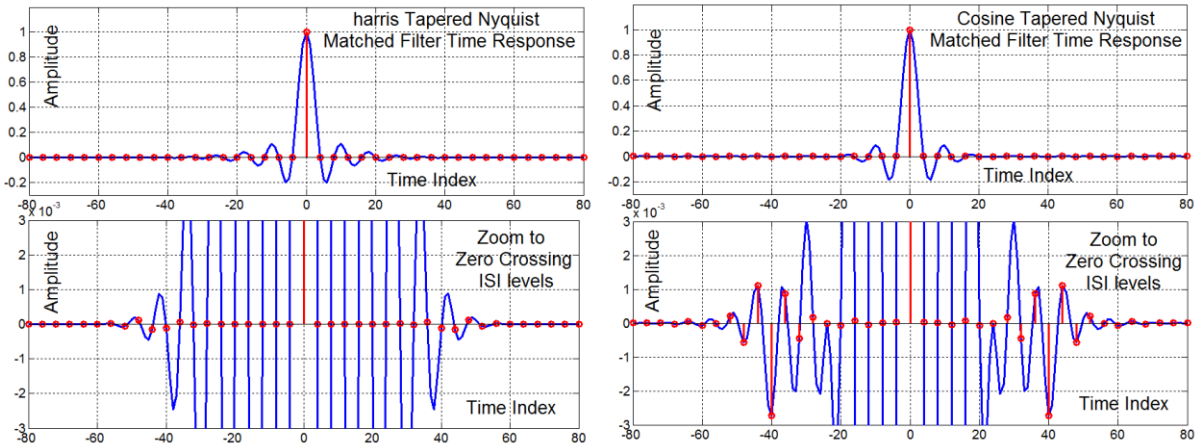

Figure 5. Matched Filter Time Responses, harris Taper and Cosine Taper SQRT Nyquist Filters: Overall Response and Zoom to Low Level Zero Crossings Detail

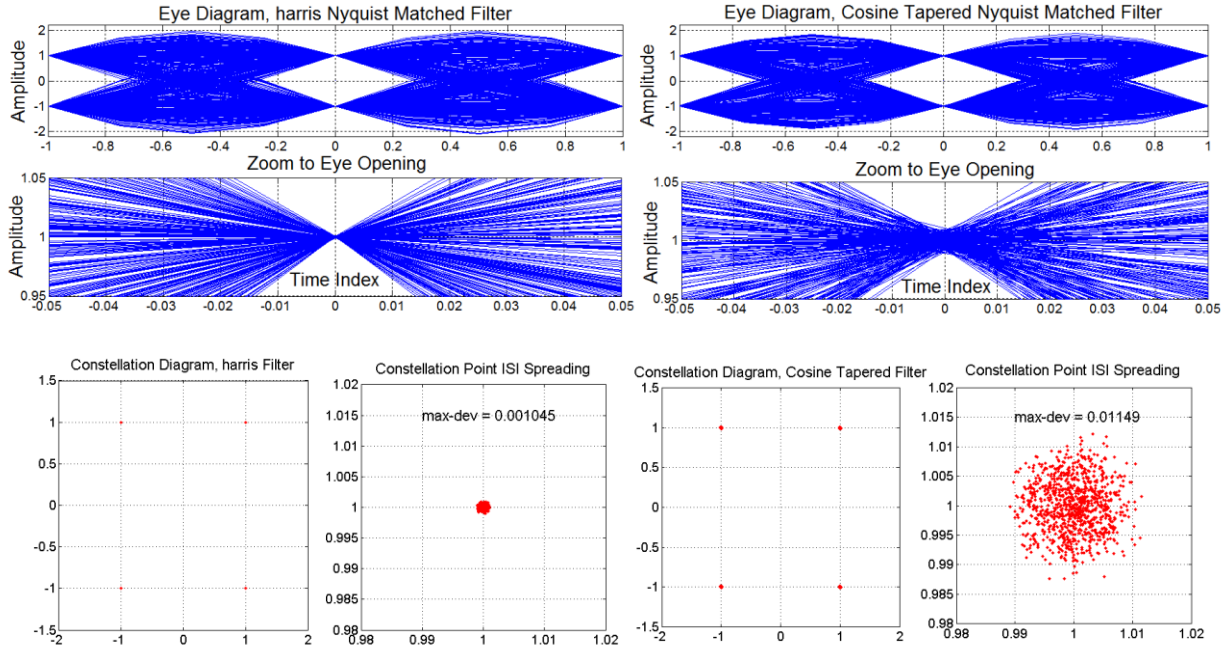

Figure 6. Comparison of harris Taper and Cosine Taper SQRT Nyquist Matched Filter Time Response Eye Diagrams, Zoom to Eye Opening, Constellation Diagrams, Overall Responses and Zoom to Fine Details

windows for spectrum analysis and filter design applications. The window should have a Fourier transform with a narrow mainlobe width and with very small sidelobe levels. We know a number of windows that satisfy this requirement. A word of caution: we are not seeking a window with minimum time-bandwidth product, but rather a window with finite support whose spectrum has a minimum mainlobe spectral width for specified spectral sidelobe levels. This will keep us from misapplying a Gaussian window to this application. Other, more appropriate windows are the Kaiser-Bessel window, the Dolph-Tchebychev window, and the minimum bandwidth Remez filter.

A short MATLAB script file that implements a harris tapered SQRT Nyquist filter is presented in Table 1. The script is quite compact and was shorted to keep the line count down. Here the 2000 point array holds 500 samples of the pass band for a 4-to-1 oversampled filter and the 125 point taper realizes the 25% excess bandwidth transition interval. Note the 0.5 value at the passband boundaries required to form the sampled data Nyquist Spectrum. There are two taper options presented and both perform equally as well. Thee NN variable here is the delay in symbols between the start of the filter and its central; leak value. The current setting is NN=10 which for the 4-samples per symbol converts to 40 samples to the filter center and an 81 tap

Table 1: MATLAB Script File, harris taper SQRT Nyquist Filter

```
% harris Taper SQRT Nyquist Filter
% 4-Samples per symbol,
% Excess BW, alpha=0.25

f0=zeros(1,2000);          % frequency array
BW=[0.5 ones(1,499) 0.5];% passband bins
f0(1001+(-250:+250))=BW; % BW in array

f1=kaiser(125,12.7)';    % taper, option 1

% ff=[0 0.000001 4.2/125 0.5]/0.5;
% gg=[1 1 0 0];
% f1=remez(124,ff,gg);    % taper, option 2

f1=f1/sum(f1);           % scale, unit area
f2x=conv(f0,f1);         % apply window
f2=f2x(63:2062);         % discard transient
f3=sqrt(f2);             % SQRT spectrum
f4=fftshift(f3);         % shift DC to bin 0

h4=4*fftshift(real(ifft(f4))); % Time series
NN=10;                   % causal delay
h5=h4(1001+(-4*NN:4*NN));% select 81 samples
h6=rcosine(1,4,'sqrt',0.25,NN);  % compare
```

filter. NN can be increased. The h5 line extracts the 81 taps from the designed harris taper SQRT Nyquist filter. The h6 line forms the same length cos taper SQRT Nyquist filter. The three filters formed by this script file contributed to the time and frequency responses shown in figure 7. Here we see the spectra of the two harris taper filters which are barely distinguishable on the scale shown as well as of the cosine taper filter. We see the sidelobe levels of the harris taper filter is an order of magnitude smaller than those of the cosine filter. We also see the same ratio for the in band ripple levels of the two filters. This is to expected because the design process presented here is that of window selection and application. The passband and stopband ripple of a filter designed with windows are always equal. When we require different levels of pass band and stopband ripple we must use a frequency dependent weighting function. The harris-Moerder Filter of [6] uses the Remez algorithm to access this option.

4 REFERENCES

[1] John Proakis, "Digital Communications", Fourth Edition, 2001, McGraw-Hill, Ch. 9.2, pp. 554-561.

[2] fred harris, "Multirate Signal processing for Communication Systems", 2004, Prentice-Hall, Ch. 4.1-4.4, pp. 82-97

[3] Sanjit Mitra and James Kaiser, "Handbook for Digital Signal processing", 1993, John Wiley & Sons, Ch. 4.8, pp. 198-214

[4] Ashkan Ashrafi and fred harris, "A Novel Square-root Nyquist filter design with prescribed ISI energy, Elsevier Signal Processing,

[5] Farhang-Boroujeny, A square-root Nyquist filter design for digital Communication systems, IEEE Transactions on Signal Processing 56 (5), 2127–2132, 2008

[6] fred.harris, Chris Dick, Karl Moerder, Sridhar Seshagiri, An improved square-root Nyquist shaping filter, Software Defined Radio, SDR'05, 2005, pp. 15–17.

[7] Ashkan Ashrafi and fred harris, A Novel Square Root Nyquist Filter Design with Prescribed ISI Energy, Elsevier Signal Processing 93, pp2626-2635, 2013

[8] fred harris, On the use of Windows for Harmonic Analysis with the Discrete Fourier Transform, Proceedings of the IEEE 66 (1), 208-221, 1978

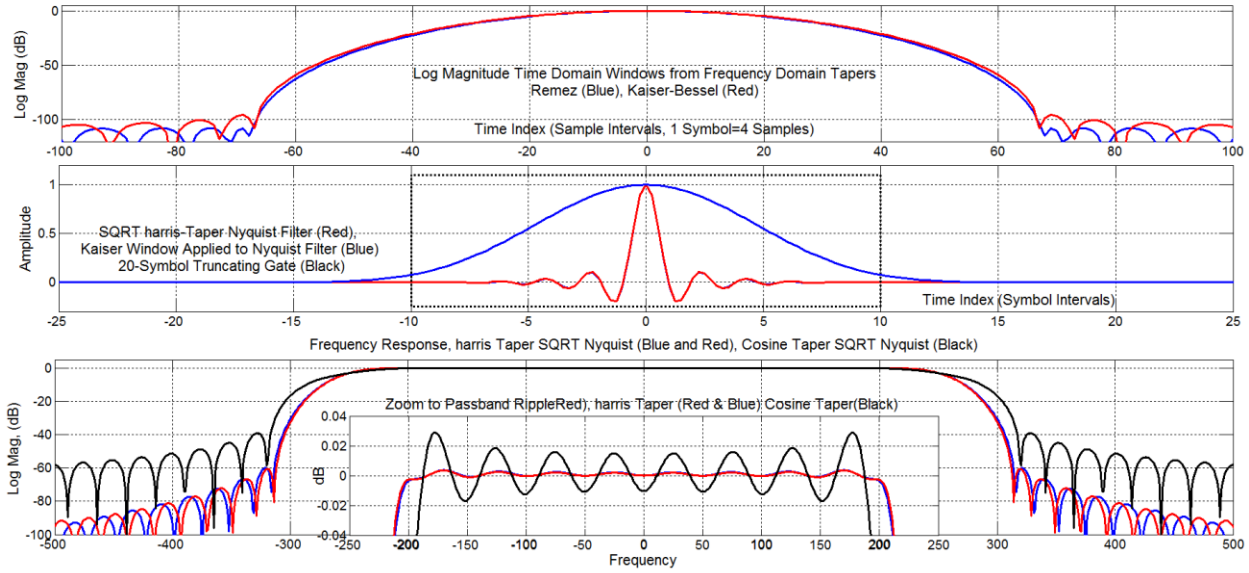

Figure 7. Log Magnitude, Inverse Transform of Frequency Domain Tapers, Linear Magnitude of Inverse Transform of Frequency Domain Tapers, harris Taper SQRT Filter Time Response, and 20 Symbol Gating Pulse. Spectra of Two 20 Symbol harris Taper SQRT Nyquist Filters and Cosine Taper SQRT Nyquist filter. Zoom to In Band Ripple of SQRT Nyquist Filters.